Extended Abstracts of the 2002 International Conference on Solid State Devices and Materials, Nagoya, 2002, pp. 710-711

A-9-4

Effects of Metal Concentration Nonuniformity in Gate Dielectric Silicates on Propagation Delay Time of CMIS Inverters

Mizuki Ono[1], Tsunehiro Ino[1], Masato Koyama[1], Akira Takashima[2], and Akira Nishiyama[1]
[1]Advanced LSI Technology Laboratory, [2]Environmental Engineering and Analysis Center,
Corporate R & D Center, Toshiba Corporation
8 Shinsugita-cho, Isogo-ku, Yokohama 235-8522 Japan
Phone: +81-45-770-3693, Fax: +81-45-770-3578, e-mail: m-ono@amc.toshiba.co.jp

Abstract

Influences of dielectric constant nonuniformity induced by nonuniform metal concentration in gate dielectric silicates on the average film dielectric constant and transistor characteristics were studied with a physical model that took polarization into account and 3-dimensional device simulations. The experimental results were compared to the calculation. It is shown that dielectric constant nonuniformity in gate dielectrics induces an increase in the propagation delay times for any metal concentration studied.

1. Introduction

As the demand for high-speed and low-power operation increases, device feature size is reduced and power supply voltage is lowered [1,2]. According to this trend, gate dielectrics are being thinned and it is estimated that they will become 1 nm for 35 nm MOSFETs [3]. In order to avoid the drastic leakage current increase that is inherent in SiO_2 gate dielectrics, high-k materials for gate dielectrics are being intensively investigated [4]. It is well-known that $Hf(Zr)O_2$ separates out and crystallize during high temperature process, resulting in nonuniformity in metal silicates [5] (Fig.1). We investigated the influences of such nonuniformity in metal concentration in gate dielectrics on MISFETs' electrical characteristics such as current drivability and propagation delay time using a physical model and 3-dimensional device simulations (DIAMOND). An experiment was conducted in order to verify the average film dielectric constant calculation.

2. Approximation to Propagation Delay Time

In this study, propagation delay time (τ_{pd}) is estimated with CV/I, where C is the load capacitance, V is the power supply voltage, and I is the saturation current. Under an approximation for parasitic effects to be negligible, both C and I are proportional to gate capacitance values. However, dielectric constant nonuniformity affects them in a different way.

3. Estimation of Load Capacitance

In order to calculate load capacitances, the average dielectric constant over films (ε_{av}) is used. In order to calculate ε_{av}, nonuniform dielectric films are modeled with a slab (dielectric constant: ε_1) containing globes (dielectric constant: ε_2). Centers of the globes are on the equidistance plane from both surfaces of the slab. Considering a depolarization field, Lorentz field, and a field of mirror charge, ε_{av} was calculated as follows:

$$\varepsilon_{av} = \varepsilon_1 \left[1 + \frac{\frac{4(\varepsilon_2 - \varepsilon_1)}{2\varepsilon_1 + \varepsilon_2} \pi \left(\frac{R}{T}\right)^3 (nT^2)}{1 - \frac{4(\varepsilon_2 - \varepsilon_1)}{2\varepsilon_1 + \varepsilon_2} \zeta(3) \left(\frac{R}{T}\right)^3} \right], \tag{1}$$

where R is the globe radius, T is the slab thickness, n is the number density of the globes, and $\zeta(3)(=1.202..)$ is the Riemann's zeta function.

Dependences of ε_{av} on a radius of globes are shown in Fig. 2(a) with average HfO_2 concentration, $\overline{X}$, as a parameter. In these calculations, nT^2 and ε_2 were set equal to 0.78 (experimental value) and 20, respectively. Here, dielectric constant of remaining $(HfO_2)_X(SiO_2)_{1-X}$ film, ε_1, was calculated with the following equation [6] which is shown in Fig.2(b):

$$\varepsilon_1 = 12 - 8.1 \times (1 - 2 \times X)^4 \tag{2}$$

For comparison, the calculated results with the following equation for ε_1, shown in Fig. 2(b), are also shown in Fig. 2(a):

$$\varepsilon_1 = 12 - 8.1 \times (1 - 2 \times X) = 3.9 + 16.2 \times X \tag{3}$$

This figure shows that the calculated ε_{av} decreases slowly with increase in radius of the globes in small radius region while it decreases rapidly in large radius region. ε_{av} increases with the radius in the case where $\overline{X} = 50\%$. In the case of low Hf concentration films, ε_1 dependence on Hf concentration is strong, resulting in rapid ε_{av} decrease with separating out of HfO_2 in large radius regions, in spite of appearance of HfO_2 region of higher-k. In the case of high Hf concentration films, ε_1 dependence on radius is weak, resulting in weak ε_{av} dependence on radius in small radius regions. In the case where $\overline{X} = 50\%$, it even increases with separating out of HfO_2. In the calculation with equation (3), ε_{av} decrease even in the case where $\overline{X} = 50\%$ and the dependence of the decreasing rate on the radius of globes is weak.

An experiment was conducted to verify the calculation. $(HfO_2)_{0.1}(SiO_2)_{0.9}$ films were sputter deposited on p-type Si (100) substrate. A post deposition annealing was performed in N_2 at 1,000°C for 30 sec. Contrary to the film without annealing (Fig. 3(a)), nonuniformity is clearly seen in the case of the film with annealing (Fig. 3(b)). HfO_2 segregation was confirmed with the detailed plain view (Fig. 4). A number density of the high-k region (n) and radii of HfO_2 (R) were estimated with Fig. 4 as 0.025 nm^{-2} and 1.4 ± 0.2 nm, respectively. The film thickness, T, was 5.6 nm, corresponding to nT^2 = 0.78. ε_{av} was measured using the accumulation capacitance at V_G = -2 V taking into consideration the effective accumulation layer thickness [7]. The measured ε_{av}'s are plotted in Fig. 2(a). ε_{av} decreases with separating out in HfO_2. Experimental results are between the 2 cases, calculated with either equation (2) or (3) and they are closer to the case calculated with equation (2) than those with (3).

4. 3-dimensional Simulations to Drive Current

In order to study drive current, 3-dimensional device simulations were carried out. The simulated devices are n-MISFETs of L/W = 35 nm/100 nm. Sources and drains with x_j of 10 nm have an overlap length between the gate and the source/drain of about 10 nm. The impurity concentration in the channel region has a maximum of 1×10^{18} cm^{-3} at a depth of 5 nm and is 1×10^{17} cm^{-3} at the substrate surface. The gate dielectric has a thickness of 3 nm and a dielectric constant of 12 (EOT = 1 nm) with $(2\ nm)^3$ cubic high-k regions with a dielectric constant of 20. The high-k regions are arranged with their centers 1.5 nm from the substrate surface and distances among themselves of 10 nm. Four MISFETs were studied; their gate dielectrics are with 0, 1, 2, and 3, rows of high-k regions, schematically shown in insets to Fig. 5, where high-k regions are shown with filled squares. V_D was set to 0.6 V [3]. The dependence of obtained I_D-V_G characteristics on the number of high-k regions is quite small (Fig.5). Potential distribution in the channel region of the device #2 at V_D = 0 V and V_G = 0.6 V is shown in Fig. 6. There are small peaks in the potential under high-k regions. It can be understood that electrical current is determined by the capacitance of the portion surrounding the small peaks.

5. Propagation Delay Time

From the results mentioned in the chapters 3 and 4, within the approximation for τ_{pd} to be CV/I, it is proportional to $\varepsilon_{av}/\varepsilon_1$, i.e., the part in the bracket of (1). Figure 7 shows dependences of CV/I on R/T with equation (2) (Fig. 7(a)) and (3) (Fig. 7(b)). Here, CV/I values are normalized with those of devices with no HfO_2 separation. This figure shows that τ_{pd} increases for all cases studied and can reach as large as 70% with nonuniform gate dielectrics such as that shown in Fig. 1. This tendency becomes stronger for larger n, smaller $\bar{X}$, and with the model using the equation (3). It is understood that τ_{pd} increase for $\bar{X}$ = 10 and 30 % is caused by the decrease in I due to ε_1 decrease and that the increase for $\bar{X}$ = 50 % is caused by the increase in C as in Fig. 2(a).

6. Conclusion

It has been shown that nonuniformity in gate dielectric increases propagation delay times. Therefore, it is indispensable to control uniformity in high-k gate dielectrics.

References

[1] M.Ono, et al., IEEE Trans. Electron Devices, **42**, p.1822 (1995)
[2] H.Wakabayashi, et al., IEDM Tech. Dig. P.49 (2000)
[3] The International Roadmap for Semiconductors.
[4] G.D.Wilk, et al., J. Appl. Phys. **89** p.5243 (2000)
[5] A.I.Kingon, et al., Nature **406** p.1032 (2000)
[6] G.Lucovsky, et al., Appl. Phys. Lett. **77** p.2912 (2000)
[7] G.Chindalore, et al., IEEE Trans. Electron Devices, **47** p.643 (2000)

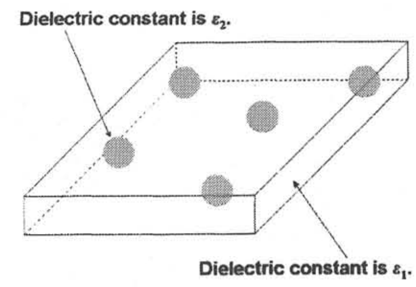

Fig.1 A schematic picture of a nonuniform gate insulator.

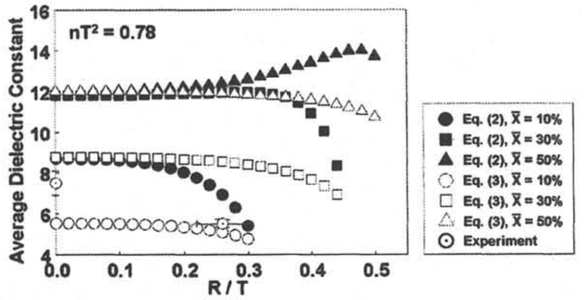

Fig.2(a) Dependences of average dielectric constant on the radius of regions having a dielectric constant of ε_2, calculated with (1) and either (2) or (3), average HfO_2 concentration, $\bar{X}$, was taken as a parameter. Experimental results for $\bar{X}$ = 10 % are also plotted.

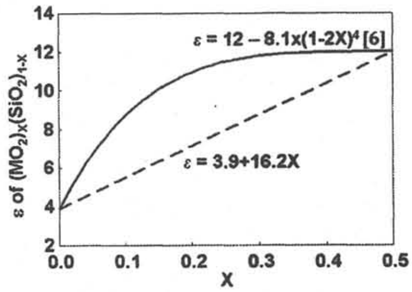

Fig.2(b) Dependences of silicate dielectric constant on Hf/ZrO_2 concentration (X), calculated with either (2) or (3).

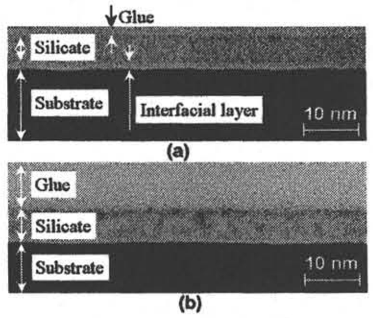

Fig.3 TEM photographs of $(HfO_2)_{0.1}(SiO_2)_{0.9}$ films (a) without and (b) with annealing process in N_2 at 1,000 °C for 30 sec.

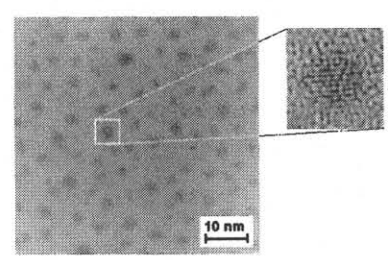

Fig.4. An in-plane TEM photograph of a $(HfO_2)_{0.1}(SiO_2)_{0.9}$ film after annealed in N_2 at 1,000 °C for 30 sec.

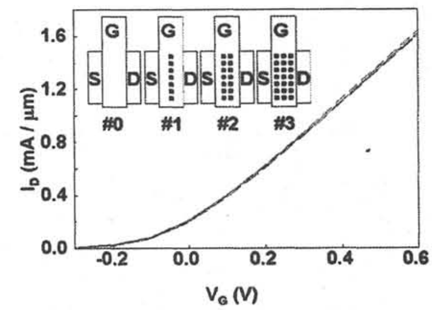

Fig.5 Simulated I_D-V_G characteristics of devices with nonuniform gate insulators.

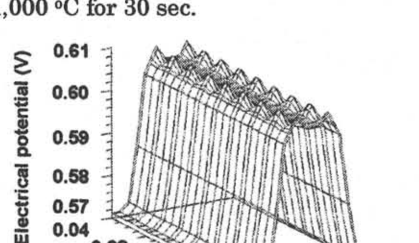

Fig.6 Potential profile in channel region of the device #2 in Fig. 5 at V_D = 0 V and V_G = 0.6 V.

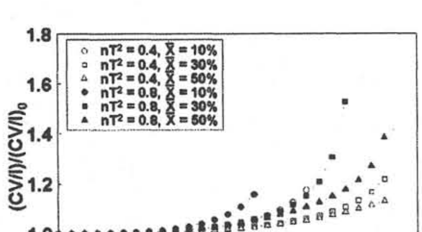

Fig.7(a) Dependences of CV/I on the radius of globes (dielectric constant: ε_2) calculated with equations (1) and (2). Here, CV/I values are normalized with those of devices with no HfO_2 separation.

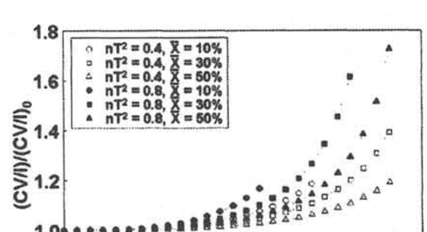

Fig.7(b) Dependences of CV/I on the radius of globes (dielectric constant: ε_2) calculated with equations (1) and (3). Here, CV/I values are normalized with those of devices with no HfO_2 separation.